Available online www.jocpr.com

Journal of Chemical and Pharmaceutical Research, 2015, 7(7):875-893

Research Article

ISSN : 0975-7384
CODEN(USA) : JCPRC5

Molecular structure, non linear optical, second order perturbation studies and thermodynamic properties of 2-(1-phenylethylidene) hydrazine carbaxamide by density functional theory

Rubarani P. Gangadharan[a], S. Sampath Krishnan[b*] and M. Thirumalai Kumar[c]

[a]*Department of Physics, Rajalakshmi Engineering College, Thandalam, Chennai, Tamil Nadu, India*
[b]*Department of Applied Physics, Sri Venkateswara College of Engineering, Chennai, Tamil Nadu India*
[c]*Department of Applied Chemistry, Sri Venkateswara College of Engineering, Chennai, Tamil Nadu, India*

ABSTRACT

The spectroscopic techniques and semi-empirical molecular calculations have been utilized to study the compound 2-(1-phenylethylidene) hydrazine carbaxamide (2PEHC). The solid phase Fourier Transform Infrared (FTIR) and Fourier Transform Raman (FTR) spectral analysis of 2PEHC is carried out along with density functional theory (DFT) calculations(B3LYP) with the 6-311++G(d,p) basis set. Detailed interpretation of the vibrational spectra of the compound has been made on the basis of the calculated potential energy distribution (PED). The individual atomic charges by NPA using B3LYP method are studied. A study on the Mulliken atomic charges, frontier molecular orbitals (HOMO–LUMO), molecular electrostatic potential (MEP) and thermodynamic properties were performed. The electric dipole moment(μ) and the first hyperpolarizability (α) values of the investigated molecule were also computed

Keywords: DFT; FTIR; FT-Raman; MEP; NBO

INTRODUCTION

Optical nonlinear conjugated organic systems have been widely studied in view of their potential application as active components in photonic and electro-optic devices [1,2]. Research in this area is focused on finding materials exhibiting large nonlinearity, fast response time, low transmission loss, and high thermal stability. Research in the field of organic NLO materials has gained momentum in the resent past on account of the interesting applications of the materials such as optical parametric amplifiers, optical parametric oscillators, Q-switched optical applications, etc. [3]. However, most of the organic NLO crystals are associated with poor mechanical strength and thermal stability [4, 5]. An organic molecule should have high second order hyperpolarizability (β) to exhibit large NLO properties. The hyperpolarizability can be enhanced by increasing intramolecular charge transfer interaction by extending the π-conjugated system [6]. The increase in conjugation length decreases the energy gap and narrows down the optical transparency window. Basically, semicarbazone family crystals exhibit nonlinear optical behavior [7, 8]. 2-(1-phenylethylidene) hydrazine carbaxamide was synthesized from the starting materials of semicarbazide hydrochloride and acetophenone using sodium acetate as a catalyst. The semicarbazides, which are the raw material of semicarbazones, have been known to have biological activity against many of the most common species of bacteria [9-11]. Semicarbazone, themselves are of much interest due to a wide spectrum of antibacterial activities [12]. Recently some workers had reviewed the bioactivity of semicarbazones and they have exhibited anticonvulsant

[13, 14], antitubercular activities [15]. To the best of our knowledge, there is no complete vibrational data on 2PEHC compound in the literature.

As per the literature study, no detailed quantum chemical computational calculations and thermodynamic properties have been performed on the chosen compound. A detailed quantum chemical investigation will aid in understanding the vibrational modes of 2PEHC and clarifying the experimental data available for this molecule. DFT calculations are known to provide excellent vibrational wave numbers scaled to compensate for the approximate treatment of electron correlation, for basis set deficiencies and anharmonicity effects [16–20]. DFT is the best method rather than the ab initio method for the computation of molecular structure, vibrational wave number and energies of molecule [21]. In this work by using the B3LYP method, vibrational wave numbers and molecular geometric parameters of 2PEHC have been calculated. These calculations are available for providing insight into the vibrational spectra and molecular parameters.

EXPERIMENTAL SECTION

The FTIR spectrum of the compound was recorded in the region 4000–400 cm^{-1} on a Perkin Elmer FTIR BX spectrometer calibrated using polystyrene bands. FT-Raman spectrum of the sample was recorded using 1064 nm line of Nd: YAG laser as excitation wave length in the region 4000–100 cm^{-1} on a Bruker RFS 100/S FT-Raman spectrometer. Spectra were collected for samples with 1000 scan accumulated for over 30 min duration. The spectral resolution after apodization was $4cm^{-1}$. A correction according to the fourth power scattering factor was performed, but no instrumental correction was done. The spectral measurements were carried out at Sophisticated Analytical Instruments Facility (SAIF), Indian Institute of Technology (IIT), Chennai.

Computational details

The quantum chemical calculations have been performed at DFT (B3LYP) methods with 6-311++G (d,p) basis sets using the Gaussian 03 program [22]. The optimized structural parameters have been evaluated for the calculations of vibrational frequencies at B3LYP method with variety of basis sets by assuming C1 point group symmetry. In order to improve the calculated values in agreement with the experimental values, a spectral uniform scaling factor was used to offset the systematic errors caused by basis set incompleteness, neglect of electron correlation and vibrational anharmonicity. Hence, the vibrational frequencies calculated at B3LYP/6-311++G (d,p) level are scaled by 0.958 for the wave numbers above 1700 cm^{-1} and for below 700 cm^{-1} scaled as 0.983 [23,24]. After scaled with the scaling factor, the deviation from the experiments is less than 10 cm^{-1} with a few exceptions. The assignments of the calculated normal modes have been made on the basis of the corresponding PEDs. The NBO calculations [25] were performed using NBO 3.1 [26] program as implemented in the Gaussian 03W package at the DFT/B3LYP level in order to understand the intra-molecular delocalization or hyper conjugation.

RESULTS AND DISCUSSION

4.1 Predictions of Raman intensities

The Raman activities (Si) calculated by Gaussian 03 program have been suitably adjusted by the scaling procedure with MOLVIB and subsequently converted to relative Raman intensities (Ii) using the following relationship derived from the basic theory of Raman scattering [27, 28].

$$\mathrm{Ii}=\frac{f(\upsilon_o-\upsilon_i)^4 S_i}{\upsilon_i[1-\exp(hc\upsilon_i/k_bT)]}$$

where υ_o is the exciting frequency (in cm^{-1}), υ_i is the vibrational wave number of the i^{th} normal mode, h, c and k_b are universal constants, and f is the suitably chosen common scaling factor for all the peak intensities. For the plots of simulated IR and Raman spectra, pure Lorentzian band shapes are used with full width at half maximum of 10 cm^{-1}.

4.2 Quantum chemical calculations

4.2.1 Molecular geometry

The optimized molecular structure for 2PEHC in the ground state is computed by the B3LYP calculations computed by the 6-311++G(d,p) basis set. The calculated geometrical parameters (bond lengths and bond angles) are compared with experimentally obtained X-ray Diffraction (XRD) data [29]. As the experimental values for 2PEHC

are known, the theoretically calculated values may give an idea about the geometry of the molecule changes from the DFT method of calculation. The optimized structural parameters of 2PEHC from the B3LYP/6-311++G(d,p) calculations and the XRD values are listed in Table 1, in accordance with the atom numbering scheme given in Fig. 1. The slight deviation in XRD data from the computed geometry is probably due to the fact that the inter-molecular interactions in the crystalline state are dominant. The B3LYP method leads to geometry parameters, which are close to experimental data.

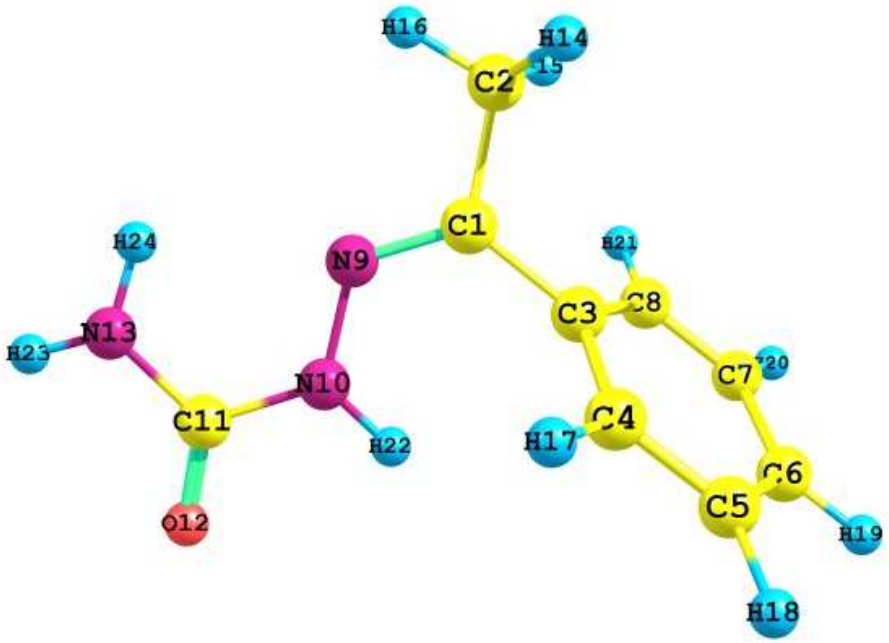

Fig 1. Numbering system adopted in the molecular structure of 2PEHC

4.2.2 Vibrational assignments

The title molecule 2PEHC with 24 atoms and 66 normal modes of fundamental vibrations has C1 point group symmetry. The calculation and visualization of contribution of internal co-ordinates in each normal mode is carried out by Gaussian 03W package [22] and Chemcraft program [30]. The internal coordinates describe the position of the atoms in terms of distances, angles with respect to an origin atom. In this study, the full sets of 89 standard internal coordinates for title compound were defined as given in Table 2. The harmonic vibrational frequencies calculated for the title compound at B3LYP level using 6-311++G (d,p) along with the observed FTIR and FTR frequencies for various modes of vibrations are presented in Table 3. The experimental and theoretically predicted FTIR and FTR spectra of 2PEHC with their scaled frequencies using scaled factors for each mode are shown in Figs. 2 and 3 respectively, for comparison. A linearity between the experimental and scaled calculated wave numbers for DFT method of 2PEHC can be estimated by plotting the calculated versus experimental wave numbers as shown in Fig. 4. The correlation coefficient (r) for experimental and observed wave numbers computed from DFT method is found to be 0.9942. It can be noted from the 'r' values that the theoretical prediction are in good agreement with the experimental wave numbers. Also, Fig. 4 reveals the over estimation of the calculated vibrational mode due to neglect of an harmonicity in real system.

Table 1 Optimized geometric parameters of 2PEHC by B3LYP/6-311++G(d,p) method

Parameter	B3LYP/6-311++G(d,p)	experimental
Bond length (A°)		
C1-C2	1.505	1.5
C1-C3	1.495	1.483
C1-N9	1.285	1.286
C2-H14	1.095	1.124
C2-H15	1.095	1.124
C2-H16	1.09	0.93
C3-C4	1.402	1.525
C3-C8	1.401	1.392
C4-C5	1.393	1.376
C4-H17	1.084	1.116
C5-C6	1.393	1.392
C5-H18	1.084	1.116
C6-C7	1.393	1.371
C6-H19	1.084	1.118
C7-C8	1.392	1.37
C7-H20	1.084	1.118
C8-H21	1.084	0.93
N9-N10	1.36	1.387
N10-C11	1.392	1.335
N10-H22	1.014	1.011
C11-O12	1.22	1.236
C11-N13	1.364	1.362
N13-H23	1.005	0.997
N13-H24	1.007	0.99
Bond angle(A°)		
C2-C1-C3	118	118.67
C2-C1-N9	117.39	117.5
C3-C1-N9	124.59	123.66
C1-C2-H14	110.69	110.83
C1-C2-H15	111.11	110.42
C1-C2-H16	110.14	110.52
H14-C2-H15	106.79	108.02
H14-C2-H16	109.22	108.46
H15-C2-H16	108.78	108.07
C1-C3-C4	120.64	120.07
C1-C3-C8	120.58	120.42
C4-C3-C8	118.75	117.82
C3-C4-C5	120.56	121.83
C3-C4-H17	119.62	119.6
C5-C4-H17	119.8	119.6
C4-C5-C6	120.17	120.23
C4-C5-H18	119.68	117.82
C6-C5-H18	120.13	120.76
C5-C6-C7	119.71	119.8
C5-C6-H19	120.14	120.23
C7-C6-H19	120.13	120.76
C6-C7-C8	120.18	120.2
C6-C7-H20	120.09	120.3
C8-C7-H20	119.72	119.8
C3-C8-C7	120.59	120.2
C3-C8-H21	119.76	119.5
C7-C8-H21	119.63	119.63
C1-N9-N10	120.16	120.55
N9-N10-C11	121.42	121.74
N9-N10-H22	122.09	120.33
C11-N10-H22	115.66	115.35
N10-C11-O12	120.32	120
N10-C11-H13	114.82	111.83
O12-C11-H13	124.81	123.27
C11-H13-H23	116.57	112.3
C11-H13-H24	119.42	-
H23-H13-H24	120.24	-

Table 2 Definition of internal coordinates of 2PEHC

No.	Symbol	Type	Definition
Stretching			
1-2	νi	C-C(Chain)	C1-C3,C1-C2
3-8	νi	C-C(Ring)	C3-C8,C8-C7,C7-C6,C6-C5,C5-C4,C4-C3
9-13	νi	C-H(Ring)	C8-H21,C7-H20,C6-H19,C5-H18,C4-H17
14-16	νi	C-H(methyl)	C2-H16,C2-H14,C2-H15
17-18	νi	C-N	C11-N13,C11-N10
19	νi	C=O	C11-O12
20-22	νi	N-H	N13-H23,N13-H24,N10-H22
23	νi	C=N	C1-N9
24	νi	N-N	N9-N10
Bending			
25-30	βi	C-C-C	C3-C4-C5,C4-C5-C6,C5-C6-C7, C6-C7-C8,C8-C3-C4,C7-C8-C3
31-40	βi	C-C-H	C3-C4-H17,C5-C4-H17,C4-C5-H18, C6-C5-H18,C5-C6-H19,C7-C6-H19, C6-C7-H20,C8-C7-H20,C7-C8-H21, C3-C8-H21
41-42	βi	C-C-N	C3-C1-N9,C2-C1-N9
43-45	βi	C-C-H	C1-C2-H14,C1-C2-H15,C1-C2-H16
46	βi	H-N-N	H22-N10-N9
47-49	βi	C-N-H	C11-N13-H24,C11-N13-H23,C11-N10-H22
50	βi	C-C-C	C3-C1-C2
51-52	βi	O=C-N	O12-C11-N10,O12-C11-N13
53-54	βi	C-N-N	C1-N9-N10,C11-N10-N9
55-57	βi	H-C-H	H14-C2-H15,H14-C2-H16,H15-C2-H16
58	βi	H-N-H	H24-N13-H23
59-60	βi	C-C-C	C1-C3-C8,C1-C3-C4
61	βi	N-C-N	N10-C11-N13
Out of Plane bending			
62-66	ωi	C-H	H21-C8-C7-C3,H20-C7-C6-C8,H19-C6-C7-C5, H18-C5-C6-C4,H17-C4-C5-C3
67-68	ωi	C-C	C1-C2-C3-C8,C1-C2-C3-C4
69	ωi	H-N-N-C	H22-N10-N9-C11
70	ωi	H-N-C-H	H24-N13-H23-C11
71	ωi	O-C-N-N	O12-C11-N13-N10
72-74	ωi	C-C-H-H	C1-C2-H14-H16,C1-C2-H15-H16,C1-C2-H14-H16
Torsion			
75-80	τi	C-C(Ring)	C3-C4-C5-C6,C4-C5-C6-C7,C5-C6-C7-C8, C6-C7-C8-C3,C7-C8-C3-C4,C8-C3-C4-C5
81	τi	C-C(Chain)	C8-C3-C1-C2
82-83	τi	Butterfly	N10-C11-N13-H24,N10-C11-N13-H23
84-86	τi	tCH3	C3-C1-C2-H14,C3-C1-C2-H15,C3-C1-C2-H16
87	τi	C-N	C4-C3-C1-N9
88	τi	C-N-H	C1-N9-N10-H22
89	τi	O-H	O12-C11-N13-H23

θi- in plane bending; ωi- out of plane bending; τi- torsion

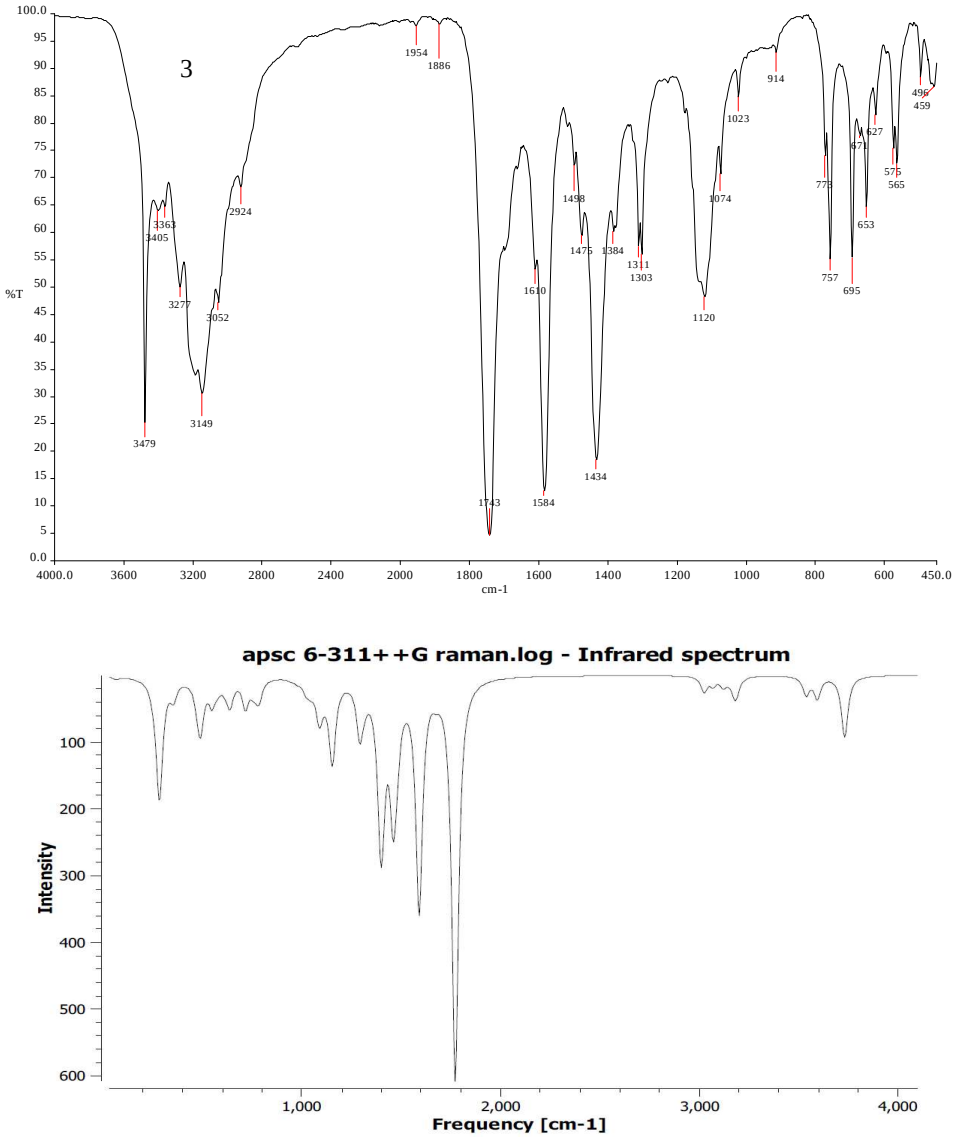

Fig 2. Comparative representation of FTIR spectra of 2PEHC

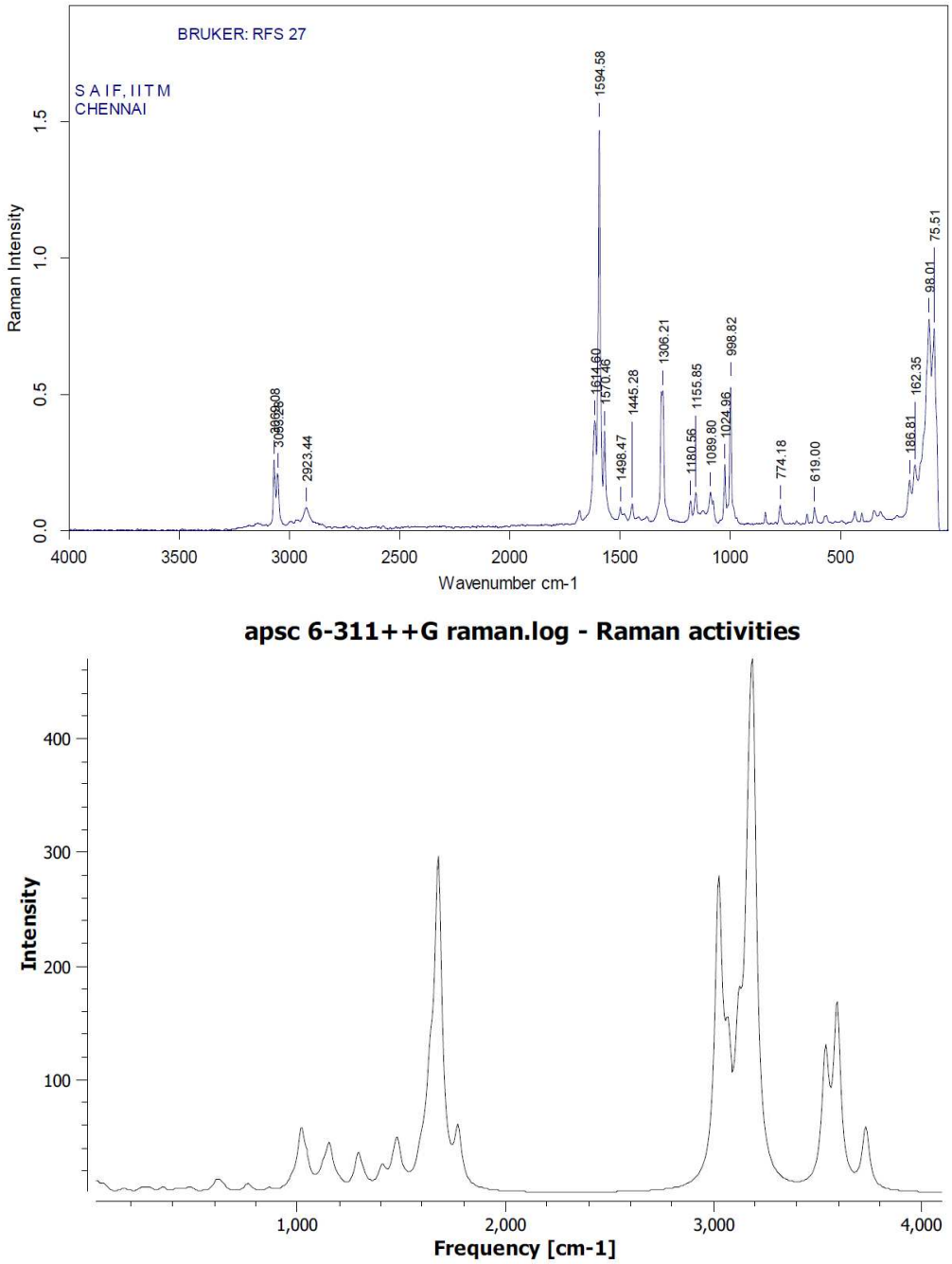

Fig 3. Comparative representation of FT-Raman spectra for 2PEHC

For the plots of simulated IR and Raman spectra, pure Lorentzian band shapes are used with a bandwidth of 40 cm^{-1}.

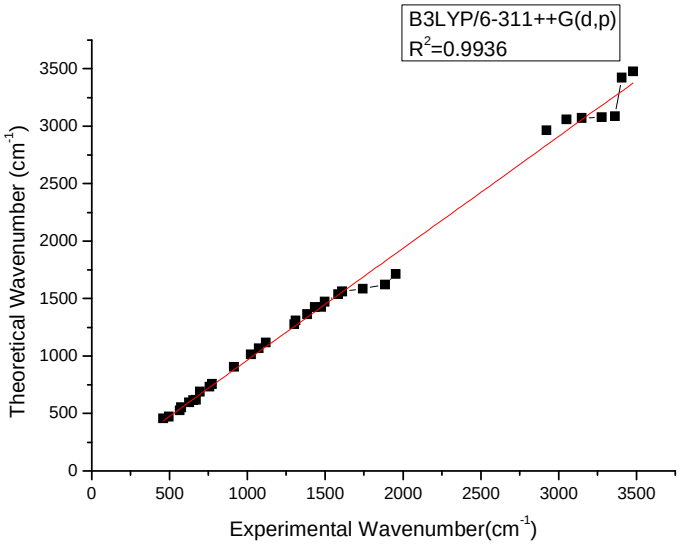

Fig 4. Correlation graph between experimental and calculated wavenumbers at B3LYP level for 2PEHC

NH_2 vibrations

The NH_2 group gives rise to the six internal modes of vibrations such as: the symmetric stretching (ν_s), the anti-symmetric stretching (ν_{as}), the symmetric deformation or the scissoring (δ), the rocking (ρ), the wagging (ω) and torsion mode (τ). The NH_2 group has two (N-H) stretching vibrations, one being asymmetric and other symmetric. The frequency of asymmetric vibration is higher than that of symmetric one. The aromatic structure shows the presence of C-H and N-H stretching vibrations above 3000 cm^{-1} which is the characteristic region for ready identification of this structure [31, 32]. These are usual range of appearance for NH_2, CH_2 and ring C-H stretching vibrations. The investigated molecule has only one NH2 group and hence one symmetric and one asymmetric N-H stretching vibrations in NH_2 group are expected. The symmetric NH_2 stretching vibration appears from 3420 to3500 cm^{-1} [33]. In this study, the FT-IR band at 3479 cm^{-1} have been assigned to NH_2 symmetric stretching vibrations. The scaled vibrations calculated at 3609 cm^{-1} and 3476 cm^{-1} by B3LYP/6-311++G (d,p) method which are listed in Table 3 correspond to asymmetric stretching mode of NH units with the PED contribution of 100% and 96%, respectively. The scaled vibration calculated at 3422 cm^{-1} by B3LYP/6-311++ G(d,p) has contributions of 97% .The vibrational NH_2 scissoring deformation appears in the region 1584 cm^{-1} with strong to very strong IR intensity [34].The theoretically computed values of NH_2 scissoring give wave number at 1538 cm^{-1} by B3LYP/6-311++G (d,p) method. The experimental values are found to be in good agreement with the theoretical values.

CH_2 VIBRATIONS

The stretching modes of the CH_2 groups were recorded in the region 3255-2858 cm^{-1} [35]. The major coincidence of theoretical values with that of experimental values is found in the symmetric and asymmetric vibration of the methylene (-CH_2-) group. For the assignments of CH_2 group frequencies, basically six fundamentals can be associated to each CH_2 group namely CH_2 symmetric stretch, CH2 asymmetric stretch, CH_2 scissoring and CH_2 rocking which belongs to in-plane vibrations and two out-of plane vibrations, viz., CH_2 wagging and CH_2 twisting modes, which are expected to be depolarized. The asymmetric stretching and symmetrical stretching [36] occur, respectively, near 3463 and 2914 cm^{-1}. In this study, the FT-IR bands at 3363 cm^{-1} and FT-Raman bands at 2944 have been assigned to CH_2 asymmetric stretching vibrations, and the FT-IR bands at 3052 cm^{-1} and FT-Raman bands at 3069 cm^{-1} have been assigned to CH_2 symmetric stretching vibrations. The theoretically computed values of CH_2 asymmetric stretching give wave number at 3087 cm^{-1} by B3LYP/6-311++G(d,p) method and CH_2 symmetric stretching exhibits wave number at 3083 which coincides exactly with experimental observations. The scissoring vibration of CH_2 at 1498, 1384 cm^{-1} in FT-IR spectra and at 1445 cm^{-1} in FT-Raman spectra, twisting vibration of CH_2 at 1120 cm^{-1} in FT-IR spectra and at 1150, and 1107 cm^{-1} in FT-Raman bands are presented in Table 3.The wagging vibrations due to CH_2 group [37] at 1311, 1303 and 1023 cm^{-1} in FT-IR spectra and at1180 and 1024 cm^{-1} in FT-Raman spectra are well comparable with theoretically calculated values.

Table 3 The observed FT-IR, FT-Raman and calculated wave numbers using B3LYP method with 6-311++G(d,p) basis sets and probable assignments for 2PEHC

Mode No.	Observed frequencies(cm-1)		Calculated frequencies(cm-1)					
	FT-IR	FT-Raman			IR[a] intensity	Raman[b] activity	force constant	Vibrational Assignment (%PED)
			Unscaled	Scaled				
1			3732	3609	91.78	53.55	9.06	ν_{as} NH_2(100)
2	3479		3595	3476	32.39	154.59	7.96	ν_s NH_2(96)
3	3405		3539	3422	27.18	110.38	7.94	ν_s NH(97)
4	3363		3192	3087	11.55	325.16	6.59	ν_{as} CH_2 (93)
5	3277		3183	3078	19.09	25.24	6.53	ν_{as} CH (75)
6	3149		3176	3071	6.42	94.85	6.48	ν_{as} CH (56)
7		3069	3168	3063	0.05	95.38	6.43	$\nu_s CH_2$(93)
8	3052	3053	3163	3059	1.82	12.68	6.4	δCH_2 (10)+β CH(30)
9			3124	3021	15.2	101.2	6.32	$\nu_s CH_2$ (91)
10	2924		3066	2965	13.05	86.07	6.09	ν_s CH_2 (73)
11		2923	3021	2921	22.65	255.24	5.57	$\nu_s CH_3$ (92)
12	1954		1772	1714	602.19	45.91	13.09	ν_sC=O(25)+ β C-NH(5)
13	1886	1614	1678	1623	11.52	279.16	14.37	ν_s C=N(50)+ ν CC(14)+ δCH_2 (10)
14	1743	1594	1639	1585	0.27	71	8.66	Ring Breathing
15	1610	1570	1614	1561	1.88	11.89	8.11	Ring bending (50)
16	1584		1591	1538	343.1	17.15	1.94	δ NH_2 (83)
17	1498	1498	1523	1473	4.68	1.88	2.99	Ring deformation (46)
18		1445	1484	1435	32.49	23.08	1.67	δ CH_2 (83) + β NH(10)
19	1475		1477	1428	7.22	9.34	1.53	ω CH_2 (81)
20	1434		1473	1424	43.92	8.91	1.83	ω CH_3 (85)
21			1460	1412	158.91	6.65	2.3	δ CH_2 (81) + β NH(22)
22	1384		1412	1365	57.5	14.45	1.75	δ CH_2 (81) + β NH(10)
23			1399	1353	212.86	3.73	2.14	δ NH_2 (13) + β C-NH(5) + ρ CH_2 (13)
24	1311	1306	1354	1309	2.31	1.11	1.62	ω CH_2 (81)
25	1303		1318	1275	14.71	7.11	4.92	ω CH_2 (75)
26			1294	1251	78.69	28.82	4.12	ω CH_2 (34) + β NH(10)
27		1180	1204	1164	1.31	3.64	0.97	ω CH_2 (85)
28		1155	1184	1145	0.09	3.69	0.92	ν CC(11) + ω CH_2 (74)
29	1120		1156	1118	122.46	34.93	2.89	t CH_2 (10) + ν NH(59)
30		1089	1128	1091	5.39	13.6	1.72	t CH(21) + ν NH(5)
31	1074		1103	1067	9.23	0.39	1.16	β C-NH(7) + t CH_2 (59)
32			1090	1054	52.69	2.44	1.32	ρ NH_2 (10) + ω CH_2 (14)
33	1023	1024	1049	1014	1.22	3.17	1.04	ω CH_2 (85)
34			1046	1011	13.79	15.64	1.41	t CH_2 (65) + β CH(17)
35		998	1020	986	15.07	0.85	1.19	ρ NH_2 (49) + t CH_2 (51)
36			1015	982	2.84	48.15	3.38	Ring Breathing
37			1009	976	0.06	0.23	0.78	t CH_2 (65) + β CH(17)
38			990	957	0.26	0.58	0.79	ω CH_2 (50) + ν CC(40)
39			972	940	5.15	6.88	2.44	t CH_2 (47) + β NH(11) + ν CC(41)
40	914		937	906	1.42	0.66	0.71	t CH_2 (47)
41			861	833	0.21	2.55	0.54	β HNN(29) + t CH2(47) +ν_sC-NH2(15)
42	773		782	756	31.74	0.91	0.75	t CH_2 (54)
43	757		759	734	7.98	4.45	2.02	β O=CN(50) + ω NH_2 (25) + CH_2 (15)
44			754	729	9.12	2.36	2.3	t CH(36) + ω CH_2 (50)

45	695	714	690	42.84	0.03	0.48	Ring Breathing
46	671	639	618	2.06	3.11	1.36	β O=CN(50) + ω NH_2 (25) + tCH_2 (15)
47	653	636	615	37.05	2.05	1.11	Ring deformation(50)+ωNH_2(20)+C=N(20)
48	627	617	597	1.61	4.4	1.06	ν CH_2(70)+ βCH(20)
49		608	588	8.28	5.96	0.59	δCH_2(33)+νCH(13)+ tNH_2(10)+βC=N(10)
50	575	573	554	10.75	0.27	0.23	γ CH(40) + δ O=CN(49) + β C=N(12)
51	565	546	528	33.58	0.47	0.47	t NH_2 (5) + ρ O=CN(13) + γ CH(22)
52	496	488	472	73.57	2.49	0.15	t NH_2 (68) + ν NH(10) + β CH(4)
53	459	473	457	20.42	2.21	0.6	ρ CH_2 (84) + ν NH(5) + β C=O(10)
54		436	422	0.78	1.77	0.52	Ring deformation (46) + ρ NH_2 (16) + β C=O(10)
55		407	394	1.72	1.74	0.27	Ring bending (75)
56		354	342	26.72	4.13	0.31	t NH_2 (10) + γ NH(20) + ρ CH_2 (16)
57		299	289	2.92	1.24	0.17	ρ CH_2 (33) + ν CH(13)
58		282	273	181.08	2.76	0.05	γ NH(63) + γO=CN(20)
59		250	242	9.69	3.4	0.15	Ring bending (11) + γ NH(28)
60		195	189	0.73	0.76	0.08	ω NH_2 (80) + ω CH(5)
61		170	164	0.03	0.94	0.02	ω NH_2 (20) + ρ CH_2 (30)
62		161	156	1.16	2.41	0.03	ρ CH_2 (13) + ω NH_2 (28)
63		79	76	0.45	0.98	0.02	γ CH_2 (45) + ρ NH_2 (28) + γ O=CN(69)
64		68	66	1.19	3.88	0.016	ρ CH_2 (16) + γ O=C(30) + t NH_2 (15)
65		64	62	2.21	1.5	0.013	ρ CH_2 (25) + γ O=CN(53) + γ NH(10)
66		33	32	0.19	9.44	0.002	Ring deformation + γ NH(36)

Abbreviations: s-strong;vs-very strong;m-medium;w-weak;vw-very weak; νas- asymmetric stretching; νs- symmetric stretching; γ-out of plane bending; β- in plane bending; ω- wagging;t--twisting; δ – scissoring, ρ-rocking.

[a] *Relative absorption intensities normalized with highest peak absorption equal to 100,*

[b] *Relative activities normalized to 100.*

C-H stretching modes

The aromatic structure shows the presence of C-H stretching vibration in the region 3100-3000 cm^{-1}, which is the characteristic region for the ready identification of C-H stretching vibrations [37]. In this region, the nature of the substituents does not make any appreciable change [38]. Gunasekaran et al. [39] have reported the presence of C-H stretching vibrations in the region 3100-3000 cm^{-1} for asymmetric stretching and 2990-2850 cm^{-1} for symmetric stretching. The C-H stretching modes usually appear with strong Raman intensity and are highly polarized. In this molecule, the FT-IR band at 3277 cm^{-1} and FT-Raman band at 3071 cm^{-1} represent asymmetric stretching vibrations. The scaled vibration calculated at 3078 cm^{-1} by B3LYP/6-311++G (d,p) method which is listed in Table 3 correspond to asymmetric stretching mode of C-H units with the PED contribution of 75%. The bands corresponding to twisting and wagging vibrations of C-H group are presented in Table 3. The bands are observed at 1089 cm^{-1} in FT-Raman spectrum. This shows good agreement with computed wave number by B3LYP/6-311++G (d,p) method at 1091 cm^{-1}. The PED confirms that these vibrations are mixed mode as it is evident from Table 3 almost contributing 25%. The bands observed at 575 cm^{-1} in FT-IR have been assigned to C-H out-of -plane bending vibrations

C=N vibrations

The identification of C=N vibration is a very difficult task, since the mixing of several bands is possible in the region. Silverstein et al. [31] assigned C=N stretching absorption in the region 1342-1266 cm^{-1} for aromatic amines. The frequencies 1598-1411 cm^{-1} in both FT-IR and FT-Raman spectra have been assigned to C-N, C=N stretching vibration, respectively [40]. In this study, the bands identified at 1886 and 653 cm^{-1} in FT-IR spectra and at1614 cm^{-1} in FT-Raman spectra have been assigned to C=N stretching vibrations. The theoretically scaled wave numbers at 1623 and 615 cm^{-1} byB3LYP/6-311++G (d,p) method correspond to C=N stretching vibrations with PED 50 and 20%, respectively.

C-C Vibrations

The C-C stretching vibrations gives rise to characteristic bands in both the observed IR and Raman spectra, covering the spectral range from 1600 to 1400 cm^{-1} [41,42]. The ring carbon-carbon stretching vibrations in benzene ring occur in the region1625-1430 cm^{-1}. In general, the bands are of variable intensity and are observed at 1625-1590, 1590-1575, 1540-1470, 1465-1430 and 1380-1280 cm^{-1} from the frequency ranges given by Varsanyi[43] for the five bands in the region. In the present work, the FT-IR bands observed at 1886 cm^{-1} and FT-Raman bands observed at 1614 cm^{-1} have been assigned to symmetric C-C stretching vibrations. The theoretically scaled wave numbers at 1623 cm^{-1} cm^{-1} by B3LYP/6-311++G (d,p) method correspond to symmetric C-C stretching vibrations.

4.3 HOMO and LUMO analysis

The highest occupied molecular orbital (HOMO) and lowest unoccupied molecular orbital (LUMO) are the main orbitals that plays an important role in chemical stability. The HOMO exhibits the ability to donate an electron and LUMO as an electron acceptor serves the ability to obtain an electron. The HOMO and LUMO energy calculated by B3LYP/6-311++G (d,p) level of theory show the energy gap which reflects the chemical activity of the molecule.

Many organic molecules, containing conjugated k electrons are characterized by large values of molecular first hyperpolarizabilities, are analyzed by means of vibrational spectroscopy [44,45].In most cases, even in the absence of inversion symmetry, the strongest bands in the Raman spectrum are found to be weak in the IR spectrum and vice versa. But the inter-molecular charge transfer from the donor to acceptor group through a single–double bond conjugated path can induce large variations of both the molecular dipole moment and the molecular polarizability, making IR and Raman activity strong at the same time. The experimental spectroscopic behaviour described above is well accounted for ab initio calculations in k-conjugated systems that predict exceptionally large Raman and infrared intensities for some of the normal modes [46]. It is also observed in the title molecule the bands in FTIR spectrum have their counter parts in Raman shows that the relative intensities in IR and Raman spectra are comparable resulting from the electron cloud movement through k-conjugated framework from electron-donor to electron-acceptor groups. The analysis of the wave function indicates that the electron absorption corresponds to the transition from the ground to the first excited state and is mainly described by one-electron excitation from the HOMO to the LUMO.

Since, DFT based chemical reactivity description provides valuable information about the reactive sites for various types of attacks and orientation for benzidene [47], the same concepts have been applied for the compound in the present study. The Mulliken electronegativity (χ) [48], chemical hardness (η) and electronic potential are computed

using orbital energies of the HOMO and the LUMO at the B3LYP/6-311++G(d,p) level of theory. The ionization potential (μ) of the molecule is calculated using Koopmans's theorem [49] and is given by

$\mu = (E_{HOMO}+E_{LUMO})/2$

using Koopmans's theorem, chemical hardness is calculated using,

$\eta = (E_{HOMO} - E_{LUMO})/2$

Considering the chemical hardness, large HOMO–LUMO gap means a hard molecule and small HOMO–LUMO gap means a soft molecule [50]. One can also relate the stability of the molecule to hardness, which means that the molecule with least HOMO–LUMO gap means it is more reactive. The atomic orbital composition of the frontier molecular orbital for 2PEHC is shown in Fig. 5. The HOMO–LUMO energy of the 2PEHC calculated at the B3LYP/6-311++G(d,p) levels are tabulated in the Table 4. The Table 4 reveals that the energy gap reflects the chemical activity of the molecule. LUMO as an electron acceptor represents the ability to obtain an electron, HOMO represents the ability to donate an electron. In general, the HOMO becomes less bound while the LUMO becomes more bound. From the Table 4, it is concluded that the lowest energy gap is found at the DFT method.

HOMO Energy (E_{HOMO}) = -6.458 eV
LUMO Energy (E_{LUMO}) = -1.4000 eV
HOMO - LUMO (Energy gap) = 5.0583 eV

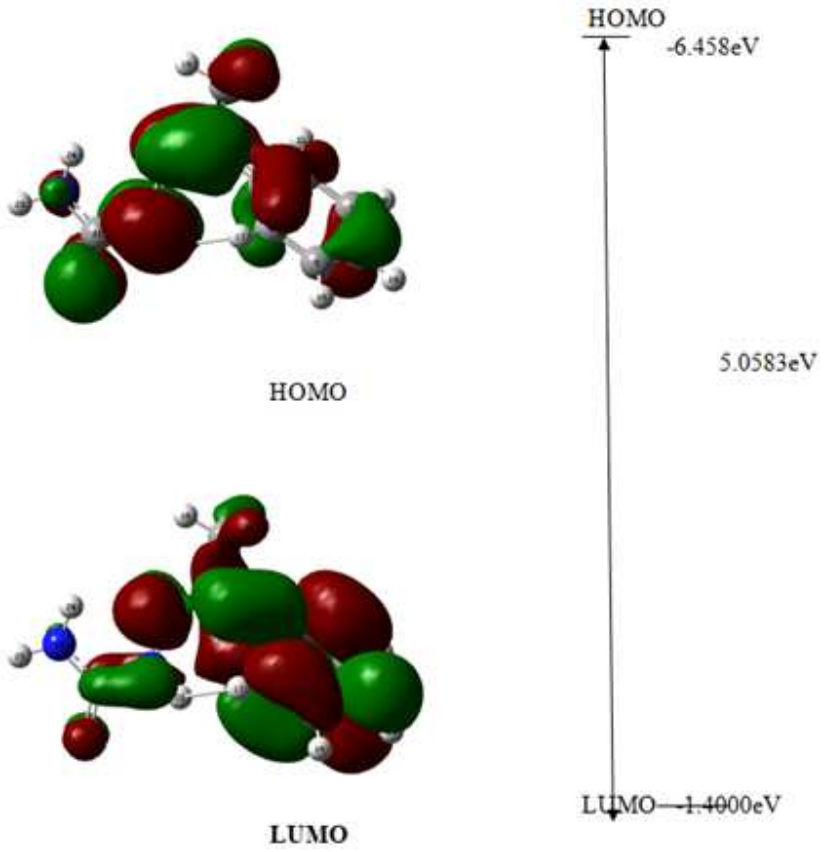

Fig. 5 The atomic orbital composition of the frontier molecular orbital for 2PEHC

Table 4 Calculated energy values of 2PEHC by B3LYP/6-311++G(d,p) method

Parameters	B3LYP/6-311++G(d,p)
SCF energy(a.u)	-589.229
Dipole moment (Debye)	1.7447
E_{HOMO}(eV)	-6.458
E_{LUMO}(eV)	-1.4
Energy gap ($E_{HOMO-LUMO}$)	5.0583
Chemical Hardness(η)	2.529
Chemical potential (μ)	-3.929
Electronegativity(χ)	3.929
Electrophilicity index (ω)	3.052
Softness(s)	0.3954

In this work Gauss-Sum 2.2 program [51] has been used to calculate group contributions to the molecular orbital's and prepare the density of the state (DOS) as shown in Fig. 6. The DOS spectra were created by convoluting the molecular orbital information with Gaussian curves of unit height. In addition, the decrease in the HOMO and LUMO energy gap explains the eventual charge transfer interaction taking place within the molecule which is responsible for the chemical activity of the molecule.

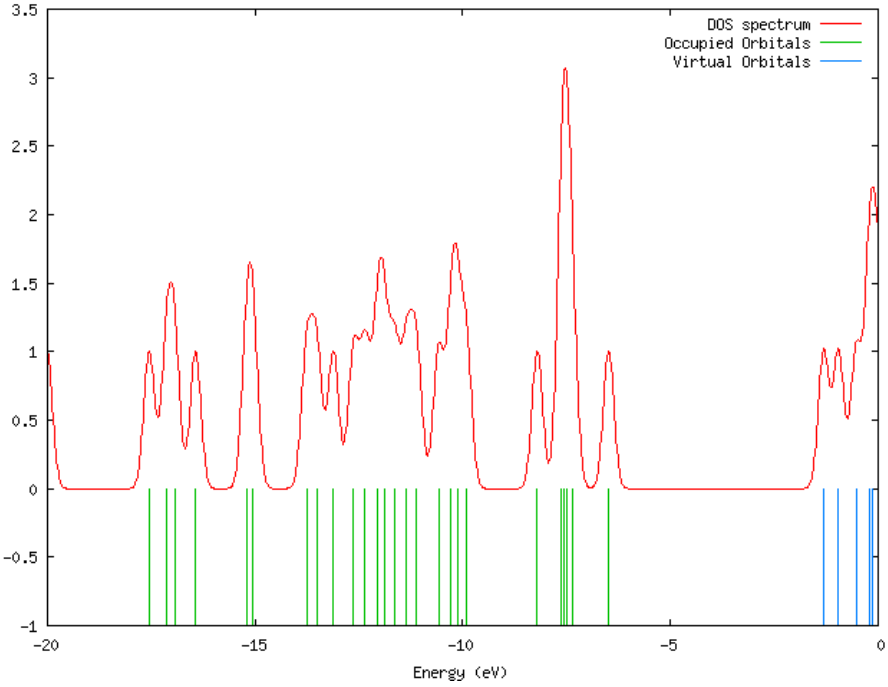

Fig 6. The calculated DOS spectrum for 2PEHC

4.4 Nonlinear optical properties and dipole moment

Density functional theory has been used as an effective method to investigate the organic non-linear optical (NLO) materials. Recent research works have illustrated that the organic non-linear optical materials are having high optical non-linearity than inorganic materials [52]. In the presence of an applied electric field, the energy of a system is a function of the electric field. Polarizabilities and hyperpolarizabilities characterize the response of a system in an applied electric field [53]. They determine not only the strength of molecular interactions but also the cross sections of different scattering and collision processes, as well as the NLO properties of the system [54,55]. For this subject, in this study the electronic dipole moment, molecular polarizability, anisotropy of polarizability and molecular first hyperpolarizability of present compound were investigated. The polarizability α and the hyperpolarizability β and the electric dipole moment μ of title compound are calculated by finite field method using B3LYP/6-311++G(d,p) basis set available in Gaussian 03 package. The polarizability and hyperpolarizability tensors (α_{xx}, α_{xy}, α_{yy}, α_{xz}, α_{yz}, α_{zz} and β_{xxx}, β_{xxy}, β_{xyy}, β_{yyy}, β_{xxz}, β_{xyz}, β_{yyz}, β_{xzz}, β_{yzz}, β_{zzz}) can be obtained by a frequency job output file of Gaussian. However, α and β values of Gaussian output are in atomic units (a.u.) so they have been converted into electronic

units (esu) (α; 1 a.u. = 0.1482 x 10^{-24}esu, β; 1 a.u. = 8.6393 x 10^{-33} esu). The complete equations for calculating the magnitude of total static dipole moment μ, the mean polarizability total α_{tot}, the anisotropy of the polarizability Δ α and the mean first hyperpolarizability β_{tot} can be calculated using the equations, respectively.

$\alpha = (\alpha_{xx} + \alpha_{yy} + \alpha_{zz}) /3$
$\Delta\alpha = 2^{-1/2}[(\alpha_{xx}-\alpha_{yy})^2+(\alpha_{yy}-\alpha_{zz})^2+(\alpha_{zz}-\alpha_{xx})^2+6\alpha^2_{xz} + 6\alpha^2_{xy} + 6\alpha^2_{yz}]^{1/2}$
$\beta_{tot} = (\beta_x^2+ \beta_y^2+ \beta_z^2)^{1/2}$
And
$\beta_x = \beta_{xxx}+ \beta_{yyy}+ \beta_{zzz}$
$\beta_y = \beta_{yyy}+ \beta_{xxy}+ \beta_{yzz}$,
$\beta_z = \beta_{zzz}+ \beta_{xxz}+ \beta_{yyz}$

Table 5 The values of calculated μ, α and β components for 2PEHC

Parameters	B3LYP/6-311++G(d,p)	Parameters	B3LYP/6-311++G(d,p)
μ_x	0.06098	β_{xxx}	-36.6528
μ_y	1.6361	β_{xxy}	9.5707
μ_z	-0.6029	β_{xyy}	51.533
μ	1.7447	β_{yyy}	202.576
α_{xx}	138.99	β_{xxz}	-29.949
α_{xy}	-10.877	β_{xyz}	-44.159
α_{yy}	146.062	β_{yyz}	-23.7535
α_{xz}	33.126	β_{xzz}	25.543
α_{yz}	-12.891	β_{yzz}	15.843
α_{zz}	129.265	β_{zzz}	-13.231
α_{total}	3.574 X 10^{-23}	β_{tot}(esu)	2.082 X 10^{-30}

The calculated values of dipole moment (μ), polarizability (α) and first hyperpolarizability (β) are tabulated in Table 5. According to the present calculations, the dipole moment and mean polarizability of 2PEHC are found to be 1.7447 D and 3.574 x 10^{-23} esu, respectively. The lowest value of dipole moment is observed for component μ_z. In this direction , this value is equal to -0.6029D. The magnitude of the molecular hyperpolarizability β, is one of key factors in NLO system. The calculated first static hyperpolarizability β_0 value is equal to 2.082 x 10^{-30} esu. Domination of particular component indicates on a substantial delocalization of charges in that direction. It is noticed that in β_{yyy} direction, the biggest values of hyperpolarizability are noticed and subsequently delocalization of electron cloud is more in that direction. The maximum β value may be due to p-electron cloud movement from donor to acceptor which makes the molecule highly polarized and the intramolecular charge transfer possible. The μ, α and β of 2PEHC are 1.7447 D, 3.574 x 10^{-23} esu and 2.082 x 10^{-30} esu, respectively, obtained by B3LYP/6-311++G (d,p) method. Urea is the prototypical molecule used in the study of the NLO properties of the molecular systems. Therefore urea was used frequently as a threshold value for comparative purposes. In this study, the total dipole moment, polarizability and the calculated β value of title molecule is greater than urea (the μ, α and β of urea are 1.3732 D, 3.8312 x 10^{-24} esu and 0.37289 x 10^{-30} esu). From the magnitude of the first hyperpolarizability of title molecule may be a potential applicant in the development of NLO materials.

4.5 NBO analysis

The NBO analysis is proved to be an effective tool for interpretation of intra- and intermolecular interaction; it also provides a convenient basis for investigating charge transfer or conjugative interaction in molecular system. The larger the E(2) (energy of hyper conjugative interactions) value, the more intensive is the interaction between electron donors and electron acceptors, i.e. the more donating tendency from electron donors to electron acceptors, the greater the extent of conjugation of the whole system. Delocalization of electron density between occupied Lewis type (bond or lone pair) NBO orbitals and formally unoccupied(anti-bond or Rydgberg) non-Lewis NBO orbitals correspond to a stabilizing donor–acceptor interaction. NBO analysis has been performed on the title molecule at the DFT/B3LYP-6311++G(d,p) level in order to explain the intra molecular, re-hybridization and delocalization of electron density within the molecule. The results of second order perturbation theory analysis of Fock matrix collected in Table 6 indicate the intra-molecular interactions due to the orbital overlap of π(C3-C4) over antibonding π*(C5-C6) with energy 19.83 kcal/mol, π(C5-C6) over π*(C3-C4) with stabilization energies 20.85 kcal/mol and π(C7-C8) over π*(C3-C4) with energies 20.62 kcal/mol. The other significant interactions in title molecule involves the interactions of LP (1) of N13 with π*(C11-O12) with stabilization energy 43.91 kcal/mol.

4.6 Molecular electrostatic potential (MEP)

The molecular electrostatic potential V(r), at a given point r(x,y,z) in the vicinity of a molecule, is defined in terms of the interaction energy between the electrical charge generated from the molecule electrons and nuclei and a positive test charge (a proton)located at r. The molecular electrostatic potential (MEP) is relatedto the electronic density (ED) and is a very useful descriptor for determining sites for electrophilic attack and nucleophilic reactions as well as hydrogen-bonding interactions [56,57]. To predict reactive sites for electrophilic and nucleophilic attack for the title molecule, molecular electrostatic potential (MEP) at the B3LYP/6-311++G(d,p) optimized geometry is calculated using the computer software Gauss view [58]. In the present study, the MEP map figure for 2PEHC molecule is shown in Fig. 7. The MEP which is a plot ofelectrostatic potential increases in the order red < orange < yellow< green < blue. The negative (red and yellow) regions of MEP were related to electrophilic reactivity and the positive (blue) regions to nucleophilic reactivity. The importance of this later lies in the fact that it simultaneously displays molecular size, shape as well as positive, negative and neutral electrostatic potential regions in terms of color grading and is very useful in research of molecular structure with its physiochemical property relationship [59–62]. The resulting surface simultaneously displays molecular size and shape and electrostatic potential value. According to the calculated result MEP shows that negatively electrophilic potential regions are mainly localized over the nitrogen atoms. However, a maximum positive region is localized on carbon atoms.

Table 6 Second order perturbation theory analysis in NBO basis for 2PEHC

Donor(i)	Type	ED(e)	Acceptor(j)	Type	ED(e)	E(2)*(kJ/mol)	E(j)-E(i)b(a.u)	F(i,j)*(a.u)
C1-C2	σ	1.97382	C1-N9	σ*	0.02062	1.72	1.23	0.041
			C3-C4	σ*	0.0254	1.6	1.18	0.039
			N9-N10	σ*	0.02589	5.86	1.03	0.069
C1-C3	σ	1.97334	C1-N9	σ*	0.02062	1.94	1.25	0.044
			C4-C5	σ*	0.01528	2.37	1.22	0.048
			C7-C8	σ*	0.01503	2.23	1.22	0.047
C1-N9	σ	1.98725	C1-C3	σ*	0.04639	1.88	1.34	0.045
			N10-C11	σ*	0.08237	1.99	1.31	0.046
			C2-H14	σ*	0.01057	2.75	0.72	0.04
	π	1.94985	C3-C4	π*	0.36468	2.53	0.36	0.029
			C2-H15	σ*	0.0104	2.36	0.72	0.037
C2-H14	σ	1.97679	C1-N9	π*	0.19825	4.62	0.52	0.046
C2-H15	σ	1.97514	C1-N9	π*	0.19825	3.54	0.52	0.04
C2-H16	σ	1.98676	C1-C3	σ*	0.04639	4.41	0.94	0.058
C3-C4	σ	1.97057	C3-C8	σ*	0.02504	3.64	1.26	0.06
	π	1.65869	C5-C6	π*	0.32439	19.83	0.28	0.067
	π		C7-C8	π*	0.31843	19.55	0.28	0.067
C3-C8	σ	1.97119	C3-C4	σ*	0.0254	3.65	1.25	0.06
C4-C5	σ	1.97904	C1-C3	σ*	0.04639	3.24	1.15	0.055
			C3-C4	σ*	0.0254	3.23	1.26	0.057
C4-H17	σ	1.97914	C3-C8	σ*	0.02504	4.53	1.08	0.062
C5-C6	π	1.65071	C3-C4	π*	0.36468	20.85	0.28	0.068
	π		C7-C8	π*	0.31843	20.14	0.28	0.068
C5-H18		1.97977	C3-C4	σ*	0.0254	4.02	1.07	0.059
C6-H19	σ	1.98037	C4-C5	σ*	0.001528	3.79	1.09	0.057
C7-C8	π	1.66016	C3-C4	π*	0.36468	20.62	0.28	0.068
			C5-C6	π*	0.32439	20.04	0.28	0.067
C7-H20	σ	1.98	C3-C8	σ*	0.02504	4	1.07	0.057
N9-N10	σ	1.98649	C1-C2	σ*	0.02029	3.22	1.28	0.057
N10-C11	σ	1.98819	C1-N9	σ*	0.02062	2.38	1.4	0.052
N10-H22	σ	1.98769	C11-N13	σ*	0.06659	3.12	1.12	0.054
C11-O12	π	1.99051	C11-O12	π*	0.35538	2.45	0.43	0.032
N13-H23	σ	1.9875	N10-C11	σ*	0.08237	3.91	1.07	0.059
N13-H24	σ	1.98696	C11-O12	σ*	0.02664	4.52	1.25	0.067
LP(1)N9	σ	1.91677	C1-C2	σ*	0.02029	11.31	0.83	0.087
LP(1)N10	σ	1.70366	C11-O12	π*	0.35538	42.65	0.31	0.105
LP(1)N10			C1-N9	π*	0.19825	31.6	0.29	0.087
LP(1)N13	σ	1.79138	C11-O12	π*	0.35538	43.91	0.32	0.11
LP(2)O12	π	1.84861	N10-C11	σ*	0.08237	24.78	0.65	0.115

ED- electron density

E(2)[a] means energy of hyper conjugative interaction(stabilization energy), [b] energy difference between donor and acceptor i and j NBO orbitals, F(i,j)[c] is the Fock matrix element between i and j NBO orbitals.

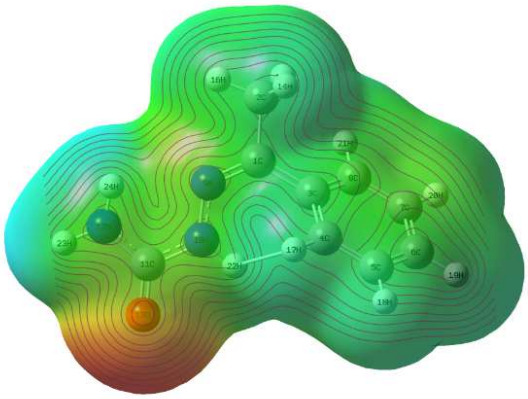

Fig. 7 Molecular Electrostatic potential (MEP) of 2PEHC

4.7 Thermodynamic properties

One of the important parameters of thermodynamics is the partition function. The partition function links thermodynamics, spectroscopy and quantum theory. The different types of partition functions are (i) translational partition function, (ii) rotational partition function, (iii) vibrational partition function and (iv) electronic partition function. Partition functions can be used to calculate heat capacities, entropies, equilibrium constants and rate constants. The total energy of a molecule is the sum of translational, rotational, vibrational and electronic energies. i.e.E = Et + Er + Ev + Ee. The statistical thermo chemical analysis of 2PEHC is carried out considering the molecule to be at room temperature of 298.15 K and one atmospheric pressure. On the basis of vibrational analysis, the statically thermodynamic functions: heat capacity $(C^0_{p,m})$, entropy (S^0_m), and enthalpy changes (ΔH^0_m) for the title molecule are obtained from the theoretical harmonic frequencies and listed in Table 7. As is evident from Table 7, all these thermodynamic values increases with the increase of temperature from 100 to1000 K, which is attributed to the enhancement of the molecular vibration while the temperature increases because at a constant pressure (db = 1 atm) values of $C_{p,m}$, S_m and H_m are equal to the quantity of temperature [63]. The correlations between these thermodynamic properties and temperatures are fitted by quadratic formulas as follows and corresponding fitting factors (R^2) for these thermodynamic properties are found to be 0.9996, 0.9999 and 0.9995 for heat capacity, entropy, and enthalpy, respectively. The temperature dependence correlation graphs are shown in Fig 8. Scale factors have been recommended [64] for an accurate prediction in determining the zero-point vibration energies, heat capacities, entropies, enthalpies.

$S^o_m = 242.91 + 0.8158T – 2 \text{ X } 10^{-4}T^2$; $R^2=0.9999$
$C^o_{p,m} = 18.538 + 0.7214T - 3 \text{ X } 10^{-4}T^2$; $R^2=0.9996$
$H^o_m = -8.2917 + 0.0946T-2 \text{ X } 10^{-4}T^2$; $R^2=0.9995$

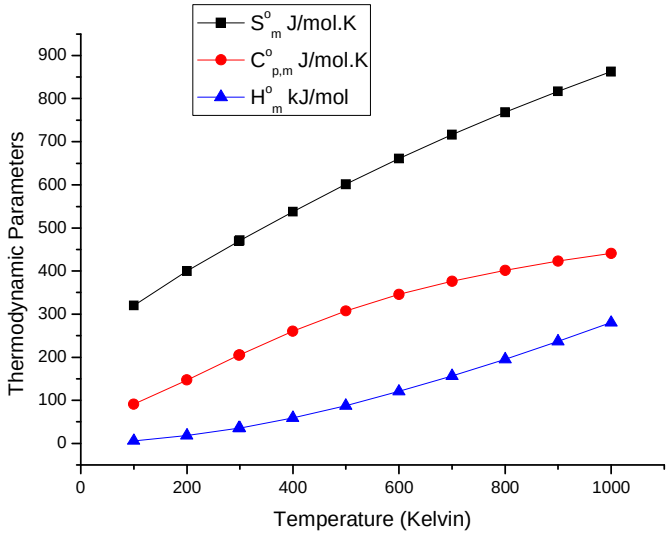

Fig 8 Correlation graph of thermodynamic parameters and temperature for 2PEHC

Table 7 Thermodynamic properties at different temperatures for 2PEHC

Temperature(K)	S°m(J/mol.K)	C°p,m (J/mol.K)	H°m (kJ/mol)
100	319.96	91.33	6.22
200	400.17	147.19	18.11
298.15	469.65	204.66	35.38
300	470.92	205.74	35.76
400	537.79	260.72	59.14
500	601.16	307.42	87.62
600	660.69	345.47	120.33
700	716.35	376.39	156.48
800	768.32	401.87	195.43
900	816.92	423.19	236.71
1000	862.47	441.26	279.96

All the thermodynamic data supply helpful information for the study of thermodynamic energies and estimate the directions of chemical reactions according to the second law of thermodynamics in the thermo chemical field[65]. It is to be mentioned that all thermodynamic calculations were done in gas phase and they could not be used in solution.

CONCLUSION

The detailed interpretation of the vibrational spectra of the 2CCHC has been performed based on the quantum mechanical approach by the B3LYP method using Gaussian program. The fitting between calculated and measured vibrational frequencies have been achieved by these methods and the deviation between calculated and experimental values is quite small after scaling frequencies. Therefore this study confirms that the theoretical calculation of the vibrational frequencies for the 2CCHC is quite useful for determining the vibrational assignment and for predicting new vibrational frequencies. The theoretically calculated values of both bond lengths and bond angles of the structures of the minimum energy have been compared with XRD data. NBO analysis was made and it is indicating the intra molecular charge-transfer between the bonding and antibonding orbitals. The lowering of the HOMO–LUMO energy gap value has substantial influence on the intra-molecular charge transfer and bioactivity of the molecule. The electric dipole moments, Mulliken atomic charges and the first hyperpolarizabilities of the compound have been calculated byB3LYP method with 6-311++G(d,p) basis set. Furthermore, the thermodynamic parameters and properties of the compound have been calculated. The correlations between the statistical thermodynamics and temperature are also obtained. It was seen that the heat capacities, entropies and enthalpies increase with the increasing temperature owing to the intensities of the molecular vibrations increase with increasing temperature.

This study demonstrates that scaled DFT/B3LYP calculations are powerful approach for understanding the vibrational spectra of medium sized organic compounds.

Acknowledgements
I sincerely thank my guide Dr. S. Sampath Krishnan, Professor and Head, Department of Applied Physics, Sri Venkateswara College of Engineering, Chennai for his invaluable guidance and support.

REFERENCES

[1] S.R. Marder, J.E. Sohn, G.D. Stucky, in: Materials for Nonlinear Optics, ACS Symposium Series 455, American Chemical Society, Washington, DC, **1991**.
[2] R.G. Denning, *J. Mater. Chem*. 11 ,**2001,** 19.
[3] Y. Mori, Y.K. Yap, T. Kamimura, M. Yoshimura, T. Sasaki, *Opt. Commun.* 1 ,**2002,** 19.
[4] H.O. Marcy, M.J. Rosker, L.F. Warren, P.H. Cunningham, C.A. Thomas, L.A. Deloach, S. Pvelsko, C.A. Ebbers, J.H. Liao, M.G. Konatzidis, *Opt. Lett.* 20 ,**1995,** 252.
[5] T. Tsunekawa, T. Gotoh, M. Iwamoto, *Chem. Phys. Lett*. 166 ,**1990,** 353.
[6] R.A. Kuijts, G.L.J. Hesselink, *Chem. Phys. Lett*. 156 ,**1989,** 209.
[7] C.C. Frazier, M.P. Cockerham, E.A. Chauchard, Chi H. Lee, *J. Opt. Soc. Am. B* 4 ,**1987,** 1899.
[8] N. Vijayan, R. Ramesh Babu, R. Gopalakrishnan, S. Dhanuskodi, P. Ramasamy, *J. Cryst. Growth* 236 ,**2002,** 407.
[9] Dogan H N, Duran A, Yemni E, *Drug Metab. Drug Interact*, **1999**, 15, 187.
[10] Hulya P, Ipek Y, Uiuk A, Feth S M, Ningur N, *J. Fac. Pharm*.,**1993**, 10,117.
[11] Cotti L, *Biochem. Terap. Sper*,1940, 27, 366, Chem. Abstr,**1943**, 37, 4421.
[12] Pandeya S N, Dimmock J R, *Pharmazie*,**1993**, 48, 659.
[13] Pandeya S N, Misra V,Singh P N, Rupainwar D C,, *Pharmacol*.,**1998**, 37,17.
[14] Pandeya S N, Yogeeswari P, Stables J P, *Eur. J. Chem*,**2000**, 35, 879.
[15] Sriram D,Yogeeswari P, Thirumurugan R S, *Bioorg. Med. Chem. Lett*, **2004**, 14, 3923.
[16] O.J. Stephens, F.J. Devlin, C.F. Chavalowski, M.J. Frisch, *J. Phys. Chem*. 98 ,**1994,** 11621–11627.
[17] F.J. Devlin, J.W. Finley, P.J. Stephens, M.J. Frisch, *J. Phys. Chem*. 99 ,**1995,** 16883–16902.
[18] S.Y. Lee, B.H. Boo, *Bull. Korean Chem. Soc*. 17 ,**1996,** 754–759.
[19] S.Y. Lee, B.H. Boo, *Bull. Korean Chem. Soc*. 17 ,**1996,** 760–764.
[20] G. Rahnut, P. Pulay, *J. Phys. Chem*. 99 ,**1995,** 3093–3100.
[21] A.D. Becke, *J. Chem. Phys*. 98 ,**1993,** 5648–5652.
[22] M.J. Frisch et al., Gaussian, Inc., Wallingford CT, **2004.**
[23] N. Sundaraganesan, H. Saleem, S. Mohan, M. Ramalingam, *Spectrochim. Acta* A 61 ,**2005,** 377–385.
[24] N. Sundarganesan, S. Ilakimani, H. Saleem, P.M. Wojaechiwsju, D. Michalska, *Spectrochim. Acta* A 61 ,**2005,** 3001–3009.
[25] J.A. Pople, H.B. Schlegel, R. Krishnan, D.J. Defrees, J.S. Binkley, M.J. Frisch, R.A. Whiteside, R.J. Hout, W.J. Hehre, *Int. J. Quantum Chem. Symp*. 15 ,**1981,** 269–278.
[26] E.D. Glendering, A.E. Reed, J.E. Carpenter, F. Weinhold, NBO Version 3.1., TCI, University of Wisconsin, Madison, **1998.**
[27] G. Keresztury, S. Holly, J. Varga, G. Besenyei, A.Y. Wang, J.R. Durig, *Spectrochim. Acta* A 9 ,**1993,** 2007–2026.
[28] G. Keresztury, in: J.M. Chalmers, P.R. Griffith (Eds.), Raman Spectroscopy: Theory in Handbook of Vibrational Spectroscopy, vol. 1, John Wiley & Sons Ltd., New York, **2002.**
[29] H.K.Fun,C.S.Yeap,M.Padaki,S.Malladi and A.M.Isloor,*Acta Cryst*.,**2009,** E65,1807-1808
[30] <http://chemcraft.com>.
[31] M. Silverstein, G. Clayton Bassler, C. Morril, Spectroscopic Identification of Organic compounds, John Wiley, Newyork, **1981.**
[32] V. Krishnakumar, R. Ramasamy, *Spectrochim. Acta Part* A 62 ,**2005,** 570-577.
[33] L.J. Bellamy, The Infrared Spectra of Complex Molecules, vol. 2, Chapman and Hall, London, **1980**.
[34] D. Lin-Vien, N.B. Colthup, W.G. Fateley, J.G. Grasselli, The Handbook of Infrared and Raman Characteristic Frequencies of Organic Molecules, Academic Press, Boston, MA, **1991.**
[35] N.P.G. Roeges, A Guide to Complete Interpretation of Infrared Spectra of Organic Structures, Wiley, NewYork, **1994.**
[36] G. Socrates, Infrared Characteristic Group Frequencies, John Wiley and Sons, New York, **1980.**

[37] G. Varsanyi, Assignments for Vibrational Spectra of Seven Hundred Benzene Derivatives, vol. 1/2, Academic Kiado, Budapset, **1973.**
[38] S. Mohan, R. Murugan, *Indian J. Pure Appl. Phys*. 31 **,1993,** 496-499.
[39] S. Gunasekaran, R. ArunBalaji, S. Seshadri, S. Muthu, *Indian J. Pure Appl. Phys*.46 ,**2008,** 162-168.
[40] N. Sundaraganesan, K. Satheshkumar, C. Meganathan, B.D. Joshua, *Spectrochim. Acta A* 65 **,2006,** 1186-1196.
[41] G. Socrates, Infrared and Raman Characteristic Group Frequencies - Tables and Charts, third ed., John Wiley & Sons, Chichester, **2001.**
[42] S. Jeyavijayan, M. Arivazhagan, *Indian J. Pure Appl. Phys*. 48 ,**2010,** 869-874.
[43] G. Varasanyi, Vibrational Spectra of Benzene Derivatives, Academic Press, Newyork, **1969.**
[44] M.A. Palofox, *Int. J. Quantum Chem*. 77 ,**2000,** 661–684.
[45] N. Sundaraganesan, G. Elango, C. Meganathan, B. Karthikeyan, M. Kurt, *J. Mol. Simul*. 35 ,**2009,** 705–713.
[46] G. Varsanyi, Assignments for Vibrational Spectra of Seven Hundred Benzene Derivatives, vol. 1 and 2, Adam Hilger, **1994.**
[47] M.A. Palafox, *Int. J. Quantum Chem.* 77 ,**2000,** 661–684.
[48] T. Vijayakumar, I.H. Joe, C.P.R. Nair, V.S. Jaykumar, *Chem. Phys*. 83 ,**2008,** 343–347.
[49] R. Parthasarathi, M. Elango, J. Padmanabhan, V. Subramanian, D.R. Roy, U. Sarkar, K. Chattaraj, *Indian J. Chem*. 45A ,**2004,** 111–125.
[50] D.A. Prystupa, A. Anderson, B.H. Torrie, J. Raman, *Spectroscopy* 25 **,1994,** 175–182.
[51] N.M. O'Boyle, A.L. Tenderholt, K.M. Langer, *J. Comput. Chem.* 29 ,**2008,** 839–845.
[52] N.B. Singh, O.P. Singh, N.P.S.N. Singh, Y.P. Singh, N.B. Singh, *Prog. Cryst. Growth Charact*. 44 (169) **,2002,** 169–174.
[53] C.R. Zhang, H.S. Chen, G.H. Wang, *Chem. Res. Chin. Univ*. 20 ,**2004,** 640–646.
[54] Y. Sun, X. Chen, L. Sun, X. Guo, W. Lu, *Chem. Phys. Lett*. 381 ,**2003,** 397–403.
[55] O. Christiansen, J. Gauss, J.F. Stanton, *Chem. Phys. Lett*. 305 ,**1999,** 147–155.
[56] N. Okulik, A.H. Jubert, *Internet Electron J. Mol. Des*. 4 ,**2005,** 17–30.
[57] E. Scrocco, J. Tomasi, *Adv. Quantum Chem*. 11 ,**1978,** 115–119.
[58] A. Frish, A.B. Neilson, A.J. Holder, GAUSSVIEW User Manual, Gaussian Inc., Pittsburgh, CY, **2009.**
[59] J.S. Murray, K. Sen, Molecular Electrostatic Potentials, Concepts and 399 Applications, Elsevier, Amsterdam, **1996.**
[60] I. Alkorta, J.J. Perez, *Int. J. Quantum Chem*. 57 **,1996,** 123–135.
[61] F.J. Luque, M. Orozco, P.K. Bhadane, S.R. Gadre, *J. Phys. Chem.* 97 ,**1993,** 9380–9384.
[62] J. Sponer, P. Hobza, *Int. J. Quantum Chem.* 57 ,**1996,** 959–970.
[63] F., J. Bopp, J. Meixner, Kestin, Thermodynamics and Statistical Mechanics, fifth ed., Academic Press Inc. (London) Ltd., New York, **1967**.
[64] G. Varsanyi, P. Sohar, *Acta Chim. Acad. Sci. Hung*. 74 ,**1972,** 315–333.
[65] R. Zhang, B. Dub, G. Sun, Y. Sun, *Spectrochim. Acta* A 75 ,**2010,** 1115–1124.